RICE UNIVERSITY

TEMPERATURE DEPENDENCE OF THE NUCLEAR SPIN-LATTICE RELAXATION TIME IN CaF_2:Nd

by

ROBERT WAYNE BURNETT

A THESIS SUBMITTED
IN PARTIAL FULFILLMENT OF THE
REQUIREMENTS FOR THE DEGREE OF
MASTER OF ARTS

Thesis Director's signature:

Harold E. Rorschach, Jr.

Houston, Texas

April 1965

Abstract

Measurements of the F^{19} nuclear spin-lattice relaxation time T_1 have been made in doped calcium fluoride over the temperature range extending from 300°K down to about 2°K. The doping element was the rare earth neodymium. Data were obtained by a pulsed nuclear resonance method for two orientations of the crystal with respect to the magnetic field.

The experimental results were analyzed by means of a general expression for T_1 valid for intermediate cases as well as for the diffusion limited and rapid diffusion limits. Dependence of the barrier radius on the temperature and the relaxation time of the paramagnetic impurity is taken into account in this expression. There is reasonable agreement between the experimental measurements and the theoretical expression over the entire temperature range.

Table of Contents

I. Introduction

Bloembergen [1] proposed a mechanism to explain the nuclear spin-lattice relaxation time in insulating crystals doped with paramagnetic impurities. In his theory, nuclear spin magnetization diffuses from nucleus to nucleus as a result of dipole-dipole coupling. In the vicinity of a paramagnetic impurity, Zeeman energy can be transferred to the lattice via the impurity through dipolar interaction between nuclear and impurity spins. He derived a diffusion equation for the magnetization which, when solved numerically, gave qualitative agreement with measured relaxation times. Later investigators [2,3,4] found analytic solutions to the diffusion equation and obtained relaxation times T_1 for limiting cases. Rorschach [5] derived a general expression for T_1 from the diffusion equation. In his paper the effective static moment of the impurity is calculated in order to make a better estimate of the barrier radius, the distance from the impurity within which spin diffusion is quenched due to Larmor frequency shifting. T_1 is a function of the temperature, the impurity spin-lattice relaxation time, the impurity concentration, and the magnetic field.

This thesis describes the results of a pulsed nuclear resonance experiment on a single crystal of calcium fluoride dilutely doped with the rare earth neodymium. Fluorine nuclei have spin 1/2 so there is no quadrupole moment, and in CaF_2 they occupy sites of cubic symmetry. EPR work [6] has indicated that the neodymium goes primarily into interstitial sites of tetragonal electric field symmetry as Nd^{3+} ions; the axis of axial symmetry is a (100) direction. The crystal field splits the $^4I_{9/2}$ ground state into five Kramers doublets,

with the first excited doublet lying about 60 cm^{-1} above the lowest doublet.

T_1 was measured from 2 degrees Kelvin to 300 degrees for two orientations of the sample with respect to the magnetic field. From T_1 the impurity spin-lattice relaxation time ρ can be calculated. Comparison of these calculated values with EPR measurements of ρ at low temperatures and theoretical predictions at higher temperatures serves as a check on the expression for T_1. At the higher temperatures ρ is too short to be measured directly by EPR. There would also be a signal to noise problem for low impurity concentrations. This method can thus provide experimental values of ρ in cases where it cannot be measured directly.

II. Nuclear Relaxation in Insulating Crystals

A. Spin Diffusion

Dipolar interactions between identical nuclei give rise to nuclear spin diffusion, a process in which mutual spin flips occur. In this way, Zeeman energy is transported to the vicinity of paramagnetic impurities where it can be given up to the lattice. The dipole-dipole interaction perturbation can be put in the form

$$\mathcal{H}_{I_1 I_2} = \frac{\gamma^2 \hbar^2}{r^3} (A + B + C + D) + h.c.$$

$$A = \frac{1}{2} I_{1_z} I_{2_z} (1 - 3\cos^2\theta_{12})$$

$$B = -\frac{1}{4} I_1^+ I_2^- (1 - 3\cos^2\theta_{12})$$

$$C = -\frac{3}{2} (I_1^+ I_{2_z} + I_{1_z} I_2^+) \sin\theta_{12} \cos\theta_{12} e^{-i\phi_{12}}$$

$$D = -\frac{3}{4} I_1^+ I_2^+ \sin^2\theta_{12}\, e^{-2i\phi_{12}}$$

h.c. = hermitian conjugate

$\bar{I}_i$ = spin of nucleus i

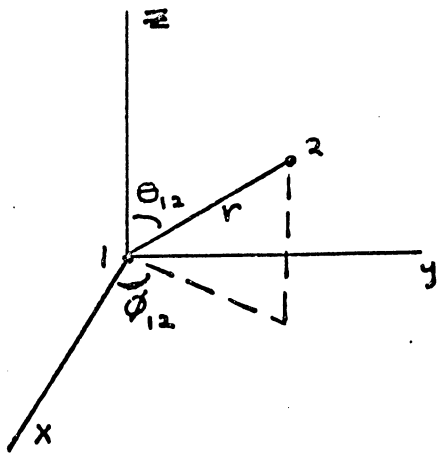

Lattice vibrations, if taken into account in terms C and D, would provide a direct mechanism for relaxation of nuclei by the lattice. However, it has been shown that this effect is negligible in comparison with the relaxing effect of paramagnetic impurities.[1] Term B is responsible for the simultaneous spin flips of two interacting nuclei. From first order time-dependent perturbation theory, we calculate a transition probability

$$W_{ij} = \frac{1}{t}\left| \langle m_i = \tfrac{1}{2},\, m_j = -\tfrac{1}{2} \left| \frac{\gamma^2\hbar^2}{r^3}(B + B^T) \right| m_i = -\tfrac{1}{2},\, m_j = \tfrac{1}{2} \rangle \times \frac{e^{-i(E_i - E_f)t/\hbar} - 1}{E_i - E_f} \right|^2 .$$

E_i and E_f are the initial and final energies.

$(E_i - E_f)/\hbar = \omega_i - \omega_j$, where ω_i is the Larmor frequency of nucleus i.

Fluctuating local fields cause a spread in Larmor frequencies.

Integrating over the frequency distribution,

$$W_{ij} = \frac{1}{10}\gamma^4\hbar^2 r_{ij}^{-6}\left(1-3\cos^2\theta_{ij}\right)^2 \lambda T_2$$

λ depends on the distribution function and is of the order of 1. T_2 is the spin-spin relaxation time.

B. Relaxation by Paramagnetic Impurities

Nuclei are relaxed by the paramagnetic impurities through a dipolar interaction $\mathcal{H}_{IS}$ between the impurity spin S and the nuclear spin I,

$$\mathcal{H}_{IS} = \frac{1}{r^3}\left[\bar{\mu}_I\cdot\bar{\mu}_S - 3\frac{(\bar{\mu}_I\cdot\bar{r})(\bar{\mu}_S\cdot\bar{r})}{r^2}\right]$$

$$\bar{\mu}_I = \gamma\hbar\bar{I}\ , \qquad \bar{\mu}_S = -\beta\,\underline{\bar{g}}\cdot\bar{S}$$

$\underline{\bar{g}}$ is the experimentally determined g tensor. The expanded form of $\mathcal{H}_{IS}$ contains terms similar to those in $\mathcal{H}_{II}$. I^+S_z will be the dominant nuclear relaxing term since this requires much less energy ($\hbar\omega_I$) than does $I^+S^{\pm}$, ($\hbar[\omega_S \pm \omega_I]$); therefore the latter term will be neglected. In Appendix A the coefficient of I^+S_z is obtained for arbitrary orientation of the magnetic field $\bar{H}$. For the orientations involved in the analysis later in this thesis, $\bar{H}$ will be either parallel or perpendicular to the impurity symmetry axis z'. If $\bar{H}\perp z'$, the term of interest is

$$\frac{\gamma\hbar\beta}{2r^3}\,3g_\perp \sin\theta\cos\theta\, e^{-i\phi} I^+S_z + h.c. \equiv K I^+S_z + h.c.$$

If $\bar{H}\parallel z'$, $g_\perp$ is replaced by $g_\parallel$.

The above interaction Hamiltonian relaxes nuclei by inducing transitions from the spin -1/2 level to the spin 1/2 level. An approximate transition probability can be derived from a semi-

classical treatment for time-dependent perturbations.[8] S_z is time-dependent because of spin flipping due to coupling with the lattice. For the case $\bar{H} \perp z'$, the transition probability is

$$W_{-\frac{1}{2}\to\frac{1}{2}} = \frac{1}{\hbar^2} \langle \tfrac{1}{2} | K I^+ + K^* I^- | -\tfrac{1}{2} \rangle \times \langle -\tfrac{1}{2} | K I^+ + K^* I^- | \tfrac{1}{2} \rangle \, J(\omega_I) .$$

$J(\omega)$ is the spectral density of S_z. A neodymium impurity ion has an effective spin of 1/2 (lowest Kramers doublet). Using this spin, it is shown in Appendix B that choosing an exponential correlation function for S_z leads to

$$J(\omega) = 2\pi \tfrac{1}{4} \tanh^2 x \, \delta(\omega) + \tfrac{1}{4} (1 - \tanh^2 x) \frac{2\rho}{1+\rho^2\omega^2}$$

$$x = \beta g_1 H / 2kT$$

For temperatures of concern in this thesis

$$J(\omega) \cong 2\pi \tfrac{1}{4} x^2 \delta(\omega) + \tfrac{1}{4} \cdot \frac{2\rho}{1+\rho^2\omega^2} .$$

Insertion into the expression for the transition probability yields the result

$$W_{-\frac{1}{2}\to\frac{1}{2}} \cong \frac{(\gamma \beta g_1)^2}{2r^6} (.3) \frac{\rho}{1+\rho^2\omega_I^2} \equiv \frac{c}{2r^6}$$

when averaged over all angles.

C. Diffusion Equation

At nucleus i, let $W_{-\frac{1}{2}\to\frac{1}{2}} = S_i$. Including both mutual spin flips and impurity-induced transitions, we can write an expression for the total probability for the transition $m_i = -\frac{1}{2} \to m_i = \frac{1}{2}$,

$$W_{i\uparrow} = \sum_{j\neq i} W_{ij} P_j Q_i + S_i Q_i$$

where P_i is the probability that $m_i = 1/2$ and Q_i is the probability that $m_i = -1/2$. Similarly,

$$W_i \downarrow = \sum_{j \neq i} W_{ij} Q_j P_i + S_i P_i$$

The magnetization density in the neighborhood of nucleus i is proportional to $P_i - Q_i \equiv n_i$. An expression for the rate of change of n_i follows from the relation

$$\frac{dP_i}{dt} = W_i \uparrow - W_i \downarrow$$

$$= \sum_{j \neq i} W_{ij} (P_j - P_i) - S_i (2P_i - 1)$$

since $P_i + Q_i = 1$. Therefore

$$\frac{dn_i}{dt} = 2 \frac{dP_i}{dt}$$

$$= \sum_{j \neq i} W_{ij} (n_j - n_i + 2) - 2 S_i n_i$$

Or,

$$\frac{dn'_i}{dt} = \sum_{j \neq i} W_{ij} (n'_j - n'_i) - 2 S_i n'_i$$

$$n'_i = n_i - n_{0i}$$

$$n_i = n_{0i} \quad \text{at equilibrium}$$

For the magnetization density $m_i = m(\bar{r}_i)$

$$\frac{dm'(\bar{r}_i)}{dt} = \sum_{j \neq i} W_{ij} [m'(\bar{r}_j) - m'(\bar{r}_i)] - 2 S_i m'(\bar{r}_i)$$

$$m'(\bar{r}) = m(\bar{r}) - m_0(\bar{r})$$

This equation can be approximated by one involving the magnetization at only one position by expanding the magnetization density

in a Taylor's series centered at $\bar{r}_i$.

$$m'(\bar{r}_j) = m'(\bar{r}_i) + \left[x_{ij} \left(\frac{\partial m'(\bar{r})}{\partial x} \right)_{\bar{r}_i} + \cdots \right]$$

$$+ \frac{1}{2} \left[x_{ij}^2 \left(\frac{\partial^2 m'(\bar{r})}{\partial x^2} \right)_{\bar{r}_i} + \cdots \right] + \cdots$$

We truncate after second order. First order terms and cross terms cancel on summing due to lattice symmetry. Also because of symmetry, the coefficients of the partial derivatives are equal, and we have finally, dropping the subscript i,

$$\frac{d\, m'(\bar{r})}{dt} = D \nabla^2 m'(\bar{r}) - C r^{-6} m'(\bar{r})$$

$$D = \sum_{j \neq i} W_{ij} x_{ij}^2$$

$$C = (\gamma \beta g_\perp)^2 (.3) \frac{\rho}{1 + \rho^2 \omega_I^2}$$

This is the diffusion equation for the magnetization derived by Bloembergen.[1]

D. Solution for the Spin-Lattice Relaxation Time

Rorschach's[5] solution of this diffusion equation for the relaxation time of the total magnetization M is

$$T_1 = (8\pi N D \alpha)^{-1} \frac{\Gamma(\frac{1}{4})}{\Gamma(\frac{3}{4})} \frac{I_{-3/4}(\delta)}{I_{3/4}(\delta)}$$

$$\frac{dM}{dt} = -\frac{1}{T_1} (M - M_0)$$

$$\delta = \frac{\alpha^2}{2b^2} \qquad \alpha^4 = C/D$$

N = impurity concentration

$I_\nu(\delta)$ is the modified Bessel function. b is the barrier radius,

the maximum distance from the impurity at which spin diffusion is quenched. Quenching occurs because the dipolar field H_p of the paramagnetic impurity shifts the Larmor frequencies of adjacent nuclei. At the distance b this shift becomes so great that mutual spin flips cannot occur. b can be estimated by setting the change in H_p over a lattice spacing a equal to the local nuclear dipolar field $\approx \mu_n/a^3$ which determines the nuclear line width:

$$\left(\frac{\partial H_p}{\partial r}\right)_b a \approx \frac{\mu_n}{a^3} .$$

$H_p \approx \frac{\mu_e}{r^3}$, where μ_e is equal to the magnetic moment of the impurity effective in quenching diffusion. We obtain for the barrier radius

$$b = a\,(3\mu_e/\mu_n)^{1/4}$$

As sketched in Appendix D, an approximate expression for μ_e is[5]

$$\mu_e^2 = \left(\frac{\beta g_\perp}{2}\right)^2 \left[\left(\frac{g_\perp \beta H}{2kT}\right)^2 + \frac{2}{\pi}\tan^{-1}\frac{2\pi\rho}{T_2''}\right]$$

if $\bar{H} \perp z'$. T_2'' is the mean lifetime of a nucleus against spin diffusion.

Combining results, the final expression for the spin-lattice relaxation time is

$$T_1 = A\left(\frac{\rho}{1+\rho^2\omega_I^2}\right)^{-1/4} \frac{I_{-3/4}(\delta)}{I_{3/4}(\delta)}$$

$$\delta = \left(\frac{\rho}{1+\rho^2\omega_I^2}\right)^{1/2} B\left(x^2 + \frac{2}{\pi}\tan^{-1}\frac{2\pi\rho}{T_2''}\right)^{-1/4}$$

$$x = \frac{\beta g_\perp H}{2kT}$$

$$A \sim N^{-1} D^{-3/4}$$

$$B \sim D^{-1/2}$$

When $\delta \ll 1$, the expression for T_1 goes over into the rapid

diffusion equation

$$T_1 = A' \left(\frac{\rho}{1+\rho^2\omega_I^2} \right)^{-1} \left(x^2 + \frac{2}{\pi} \tan^{-1} \frac{2\pi\rho}{T_2''} \right)^{3/8}$$

since $I_\nu(\delta) \rightarrow \frac{1}{\Gamma(\nu+1)} (\delta/2)^\nu$.

When $\delta \gg 1$, the diffusion limited equation obtains:

$$T_1 = A \left(\frac{\rho}{1+\rho^2\omega_I^2} \right)^{-1/4} \qquad \text{since} \quad I_{-\nu}(\delta) \rightarrow I_\nu(\delta) .$$

III. Experimental Procedure

A. Sample

The calcium fluoride sample under observation was a single crystal obtained from Harshaw Chemical Company. It was cut in the shape of a right circular cylinder with the cylindrical axis along a (100) direction. The nominal neodymium doping concentration was 0.005 weight-%.

B. Pulsed Resonance Apparatus

A receiver coil to sense nuclear signals was wound around the sample, and after x-ray alignment the unit was mounted inside a lucite sample holder. The sample holder also served as a form for the transmitter coil, oriented perpendicular to the receiver coil. This assembly was attached to the end of two thin walled stainless steel tubes which extended into a helium dewar. With a copper wire inner conductor separated from the wall of the tube by spacers, each stainless steel tube served as a coaxial cable.

Pulsed nuclear resonance apparatus capable of supplying high amplitude alternating field pulses as short as 3 microseconds was used to measure T_1. Specifically, an rf oscillator, a gated amplifier,

and a pulse sequence generator were the source of driving pulses for a kilowatt amplifier. The output of the power amplifier was coupled to the transmitter coil enclosing the sample. A 1.5 KGauss magnetic field orthogonal to both coils set the Larmor frequency at 6 megacycles per second. Nuclear induction signals were amplified and detected by a receiver designed to recover from complete saturation in about 5 microseconds. Since a short time had to be allowed for the receiver to recover from saturation, the transient signals were observed, on an oscilloscope, at a fixed time after a pulse by delayed gating. Figure 1 is a block diagram of the apparatus.

Pairs of gating pulses could be produced with variable separation between the pairs and between the pulses making up a pair. Figure 2 outlines the circuitry by which this was accomplished. These gating pulses lift the grid in the first stage of the gated amplifier from its cutoff-biased condition so that an output rf pulse can be obtained with a continuous rf oscillator input. There is negligible leakage between pulses. The pulse width was adjusted for 90 degree rotation of the magnetic moment of the nuclei (about 3 1/2 microseconds).

Further details on the apparatus can be found in the thesis by Waldrop.[7]

C. Relaxation Time Measurement

The measurement technique is based on the equation for the expectation value of the nuclear magnetic moment.[9]

$$\frac{d\langle\bar{\mu}\rangle}{dt} = \langle\bar{\mu}\rangle \times \gamma \bar{H}$$

where $\bar{H}$ is the total magnetic field at the nuclear site. Neglecting

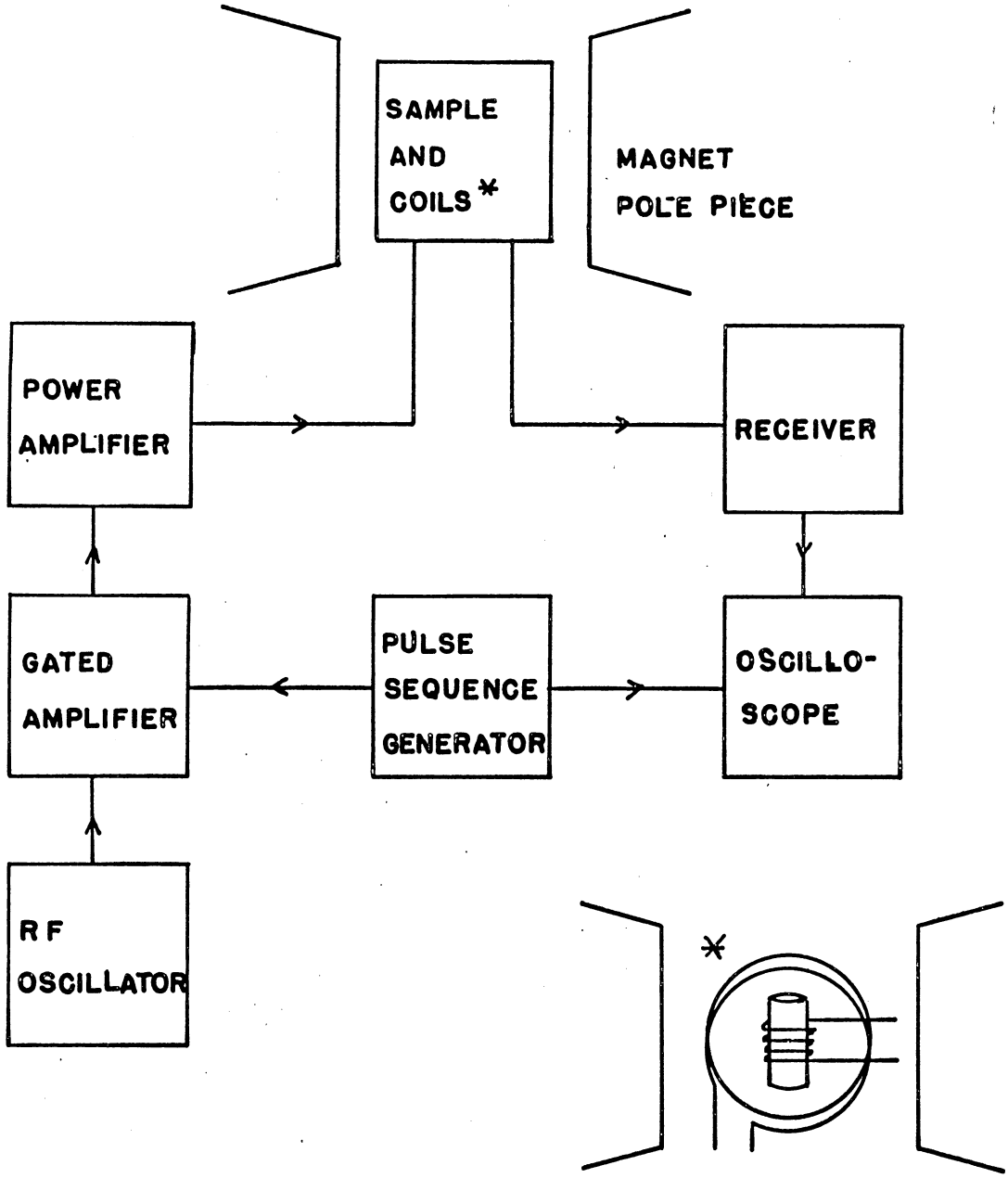

FIGURE 1

PULSED NMR APPARATUS

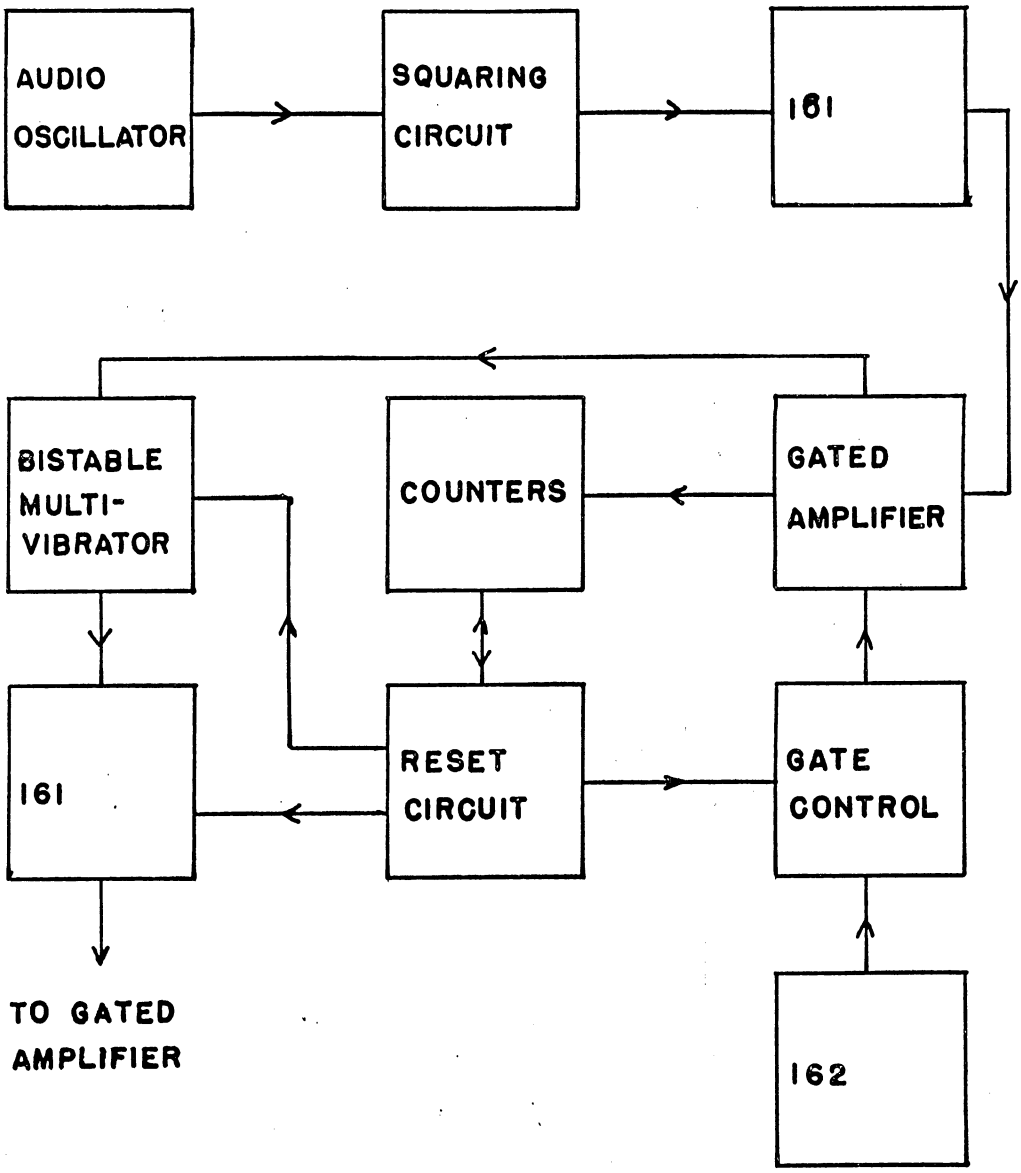

FIGURE 2

PULSE SEQUENCE GENERATOR

161: TEKTRONIX TYPE 161 PULSE GENERATOR

162: TEKTRONIX TYPE 162 WAVEFORM GENERATOR

interactions, which lead to relaxation, this equation holds for the total magnetization $\bar{M}$. It implies that $\bar{M}$ maintains a fixed angle with respect to the static magnetic field $\bar{H}$ while rotating about $\bar{H}$ at the Larmor frequency $\omega_I = \gamma H$.

If a magnetic field $2H_1 \cos \omega_I t$ alternating at the Larmor frequency is added perpendicular to the static field, $\bar{M}$ still rotates about the static field at the Larmor frequency, but the angle of inclination θ changes such that $\theta - \theta_0 = \gamma H_1 t_w$; t_w = pulse width. We take $\bar{H} \| z$. A pulse of alternating field satisfying the relation $\frac{\pi}{2} = \gamma H_1 t_w$ will rotate the magnetization vector from the equilibrium z-direction into the xy-plane. A receiver coil whose axis is in the xy-plane will then produce an induced voltage proportional to the z-component of magnetization prior to the 90 degree pulse.

Measurement cannot be made immediately after the pulse because some time must be allowed for recovery of the receiver from saturation due to the large amplitude of the transmitter pulse. While waiting for recovery, the signal voltage across the receiver coil is decaying as a result of the rapid transverse relaxation of the nuclei. However, if the shape of the decay curve is independent of the initial magnitude of the magnetization, measurements at a fixed time after the pulse will be proportional to the initial magnitude.

The procedure in determining the spin-lattice relaxation time T_1, a measure of the rate of change of M_z toward equilibrium, is to use two 90 degree pulses separated by a variable time t. Immediately after the first pulse, $M_z = 0$. The purpose of the second pulse is to measure M_z at the time t. The equilibrium value of M_z

can be determined by a measurement after a pulse separated from the previous pulse by a time long compared to T_1.

T_1 can be determined graphically from the measurements in the following way. The theory presented earlier predicts that if the magnetization deviates from the equilibrium value, it returns toward equilibrium according to the relation

$$\frac{dM_z}{dt} = -\frac{1}{T_1}(M_z - M_0).$$

Solving,

$$M_z = M_0(1 - e^{-t/T_1}).$$

Or,

$$\log(1 - M_z/M_0) = \frac{-t}{2.30T_1}.$$

Therefore, plotting $1-M_z/M_0$ versus t on semi-log paper should produce a straight line whose slope is $-1/2.30T_1$.

D. Temperature Control and Measurement

A metal helium dewar was used because it had a narrow tail for insertion between the magnet pole pieces and because it provided essential electrical shielding. Heat transfer from the tail of the dewar to liquid air in the nitrogen jacket gave a slow enough temperature drop for measurements in the 300-80 ^{o}K range. Temperatures from 80 to 4.2 degrees were obtained by controlled transfer of helium from a liquid helium storage dewar. Temperatures below 4.2 were obtained in a pumped liquid helium bath.

A copper-constantan thermocouple in good thermal contact with the sample holder was calibrated during each run at 4.2 degrees so

that between 4.2 and 80 degrees the temperature could be measured to within 0.5 degrees.[10] The reference junction was at boiling nitrogen temperature for measurements in this range and at the ice point for the measurements above 80 degrees. Helium vapor pressure measurements with a mercury manometer permitted temperature determination below 4.2 degrees. The scale used was T_{55E}.[11]

IV. Experimental Results and Analysis

Nuclear spin-lattice relaxation times T_1 were measured between 2^oK and 300^oK for two orientations of the sample with respect to the magnetic field: $\bar{H} \parallel (100)$ and $\bar{H} \parallel (110)$. These data are plotted in Figures 3 and 4; the error bar represents the estimated experimental error. The two curves are qualitatively similar, but there is a little difference in magnitude of T_1 below 4 degrees and a significant difference between 50 and 200 degrees. The behavior in the latter range is not understood. Waldrop [7] obtained similar curves for other rare earths in CaF_2 at higher doping concentrations.

Only the data for $\bar{H} \parallel (100)$ has been analyzed using the theory presented earlier. In this case, since the impurity axes lie with equal probability along any (100) direction, 2/3 of the axes are perpendicular to $\bar{H}$ and 1/3 are parallel to $\bar{H}$. For the former, the g value to use is $g_\perp$; for the latter, $g_\parallel$. If other orientations were involved, some of the theoretical development would have to be elaborated. As all angles have been averaged over, the different ion axis directions will be taken into account only by replacing $g_\perp$ by $2/3\ g_\perp + 1/3\ g_\parallel$.

Analysis requires a knowledge of the temperature dependence of

FIGURE 3

NUCLEAR RELAXATION TIME T_1 AS A FUNCTION OF TEMPERATURE; H ∥ (100).

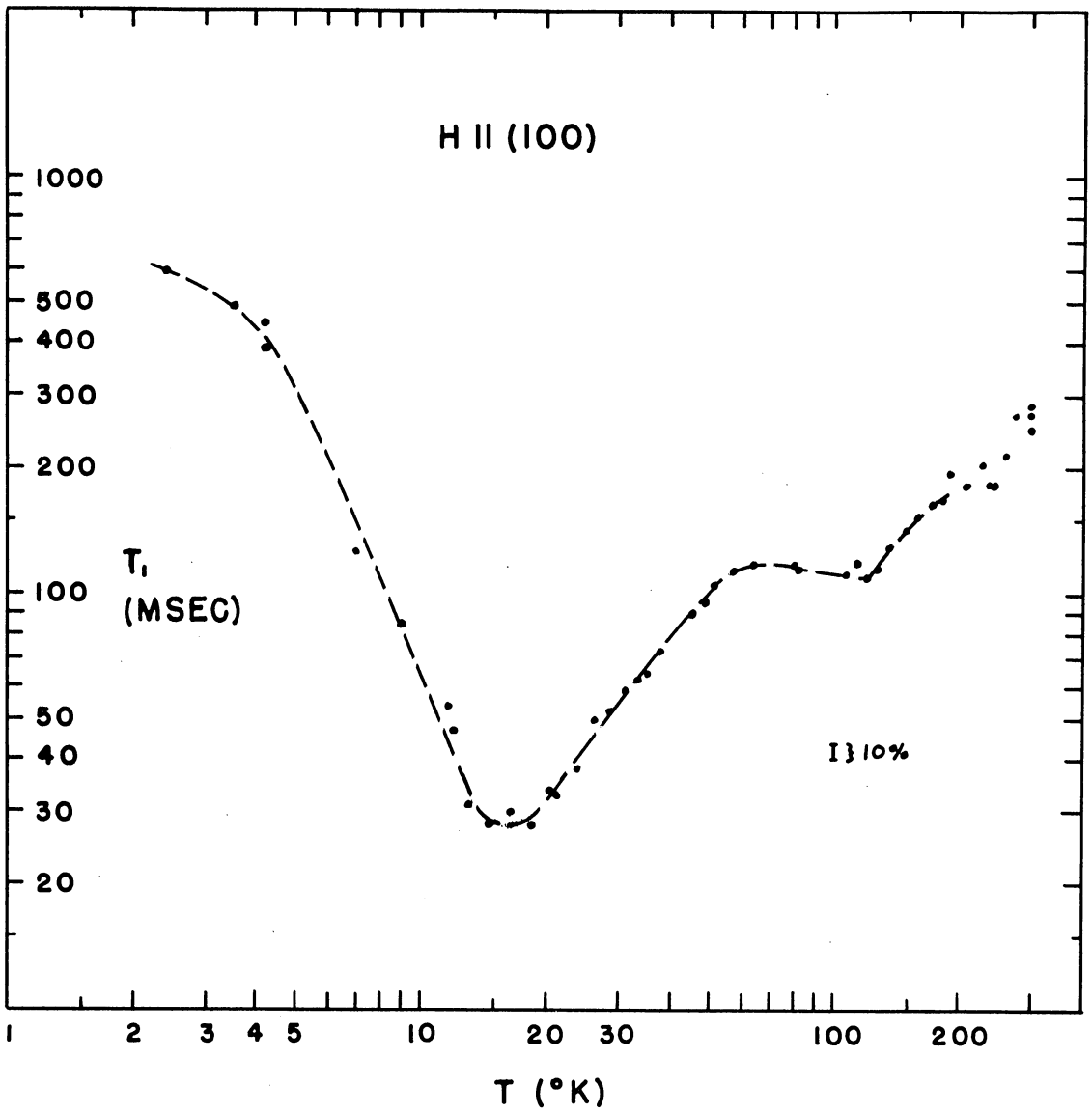

FIGURE 3

NUCLEAR RELAXATION TIME T_1

FIGURE 4

NUCLEAR RELAXATION TIME T_1 AS A FUNCTION OF TEMPERATURE; H ‖ (110).

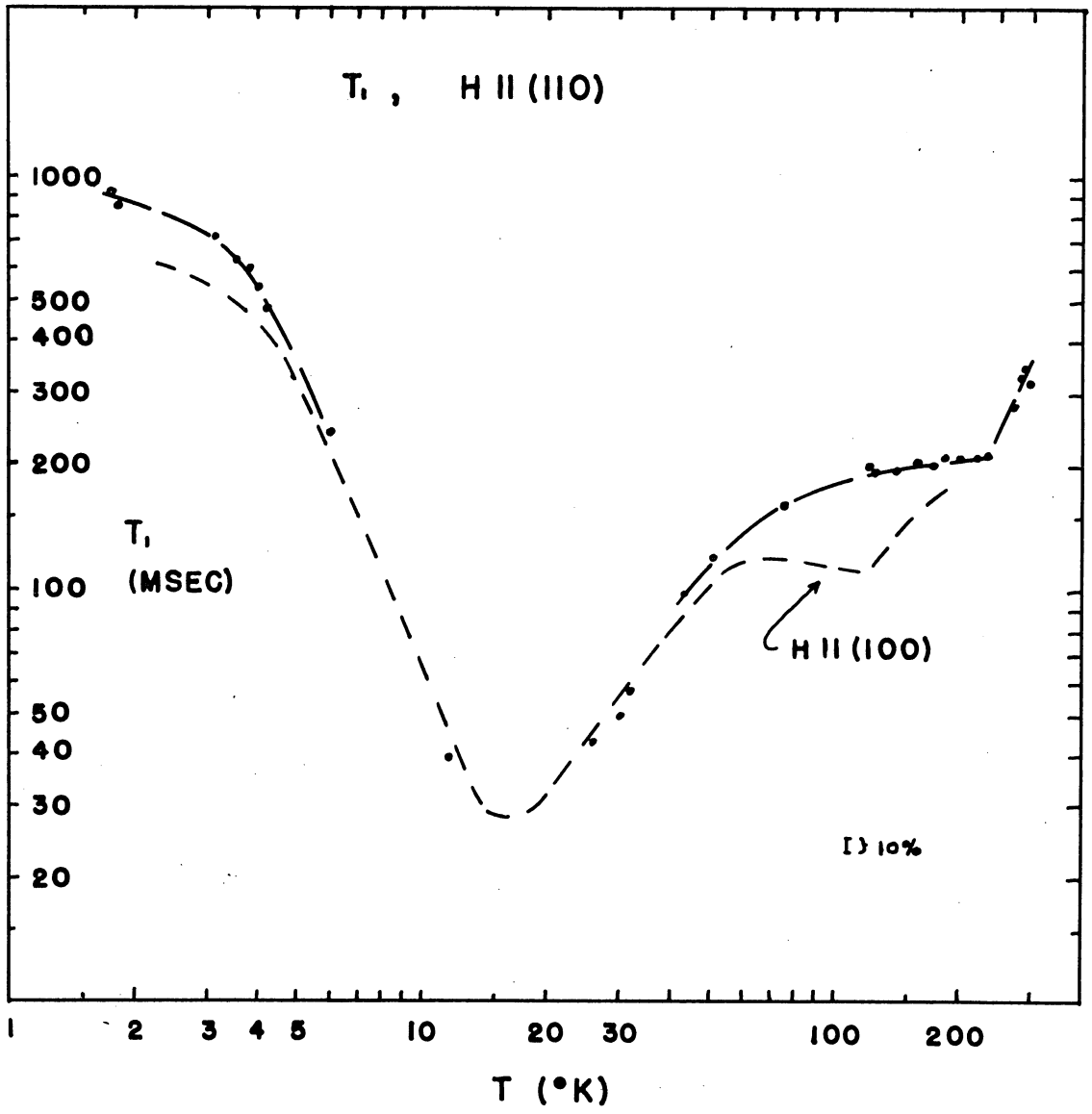

FIGURE 4

NUCLEAR RELAXATION TIME T_1

ρ , the impurity spin-lattice relaxation time. Measurements of ρ have been reported in the literature [6] for neodymium in calcium fluoride in the temperature range 2°K to 7°K. The doping concentration there was 0.28 weight-%, compared with 0.005 weight-% in this work. Only the $g_\perp$ resonance relaxation time was measured as a function of temperature, but at 2 degrees the $g_{||}$ relaxation time was also measured and was found to be twice that of the $g_{||}$ resonance. Investigation of another rare earth, cerium (Ce^{3+}), in CaF_2 reveals a concentration dependence of ρ . This concentration effect appears to be negligible below 0.2 weight-%. Theoretical work in agreement with low temperature experimental results for rare earth relaxation times predicts that ρ decreases rapidly as the temperature increases.[12,13]

Since ρ is not accurately known, the best procedure of analysis is to calculate ρ from the measured T_1 and note whether this gives values compatible with the data from the literature and with theoretical expectations. Iteration is necessary since ρ cannot be solved for directly. The expression for T_1 is

$$T_1 = A \left(\frac{\rho}{1+\rho^2\omega_I^2} \right)^{-1/4} \frac{I_{-3/4}(\delta)}{I_{3/4}(\delta)}$$

$$\delta = \left(\frac{\rho}{1+\rho^2\omega_I^2} \right)^{1/2} B \left(\frac{0.015}{T^2} + \frac{2}{\pi} \tan^{-1} \frac{2\pi\rho}{T_2''} \right)^{-1/4}.$$

A computer program was written to iterate for ρ. In this program $I_{-3/4}(\delta) / I_{3/4}(\delta)$ was evaluated either from asymptotic expressions or by interpolation between tabulated values, depending on the value of δ .

We first require estimates of the diffusion constant D and of T_2''. Considering only nearest neighbor coupling, Bloembergen obtains for a simple cubic lattice

$$\frac{1}{T_2''} = \sum_{j \neq i} W_{ij} = \frac{1}{50 T_2} .$$

Khutsishvili [2] estimates

$$D = \sum_{j \neq i} W_{ij} x_{ij}^2 = \frac{a^2}{30 T_2} .$$

Using

$$g_\perp = 1.30 \qquad T_2 \approx 3 \times 10^{-5} \text{ sec.}$$

$$g_\parallel = 4.41 \qquad a = 2.725 \times 10^{-8} \text{ cm}$$

we calculate $\beta = 4.5 \times 10^3 \, s^{-1/2}$, $\frac{2\pi}{T_2''} = 4.2 \times 10^3 \, s^{-1}$.

Since $A \sim N^{-1} D^{-3/4}$, an estimate for A is even more uncertain than for B or T_2''. A more accurate value can be obtained by setting $\frac{dT_1}{d\rho} = 0$ at 16°K, where the T_1 curve exhibits a minimum. In the diffusion limited case, this gives $\omega\rho = 1$ at the minimum, or $\rho = 2.5 \times 10^{-8} s$. In the other extreme, rapid diffusion, due to the 3/8 power dependence of $\left(\frac{0.015}{T_2} + \frac{2}{\pi} \tan^{-1} \frac{2\pi\rho}{T_2''}\right)^{3/8}$ and the relatively high temperature 16°K at the minimum, $\omega\rho = 1$ still gives a fair approximation of ρ at the minimum. This value and the measured T_1 at 16 degrees was used to calculate A.

Curve a, Figure 5, results from iterations for ρ at several temperatures between 2 and 300 degrees. Curve b is the measured data for the $g_\perp$ resonance. δ values were also recorded (Figure 6) during the calculation, and these show that the diffusion limited equation holds at temperatures near the T_1 minimum so that the relation $\omega\rho = 1$ is adequate at the minimum. ρ-calculated is seen to

FIGURE 5

IMPURITY RELAXATION TIME ρ AS A FUNCTION OF TEMPERATURE:

Curve a: ρ calculated from T_1.

Curve b: ρ measured by EPR.

Curve c: ρ calculated from T_1 after adjusting parameters.

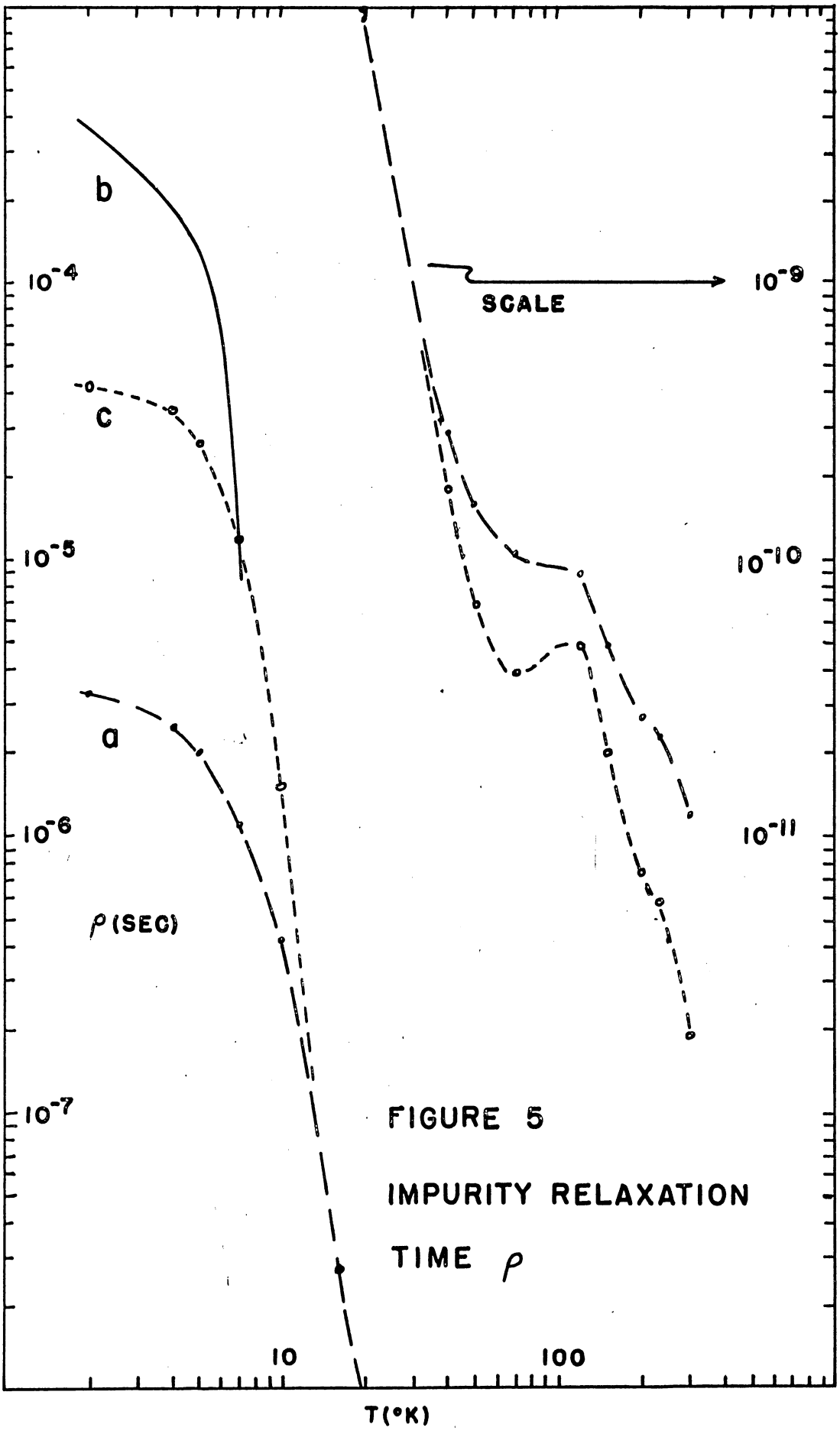

FIGURE 5

IMPURITY RELAXATION TIME ρ

FIGURE 6

BESSEL FUNCTION ARGUMENT S AS A FUNCTION OF TEMPERATURE.

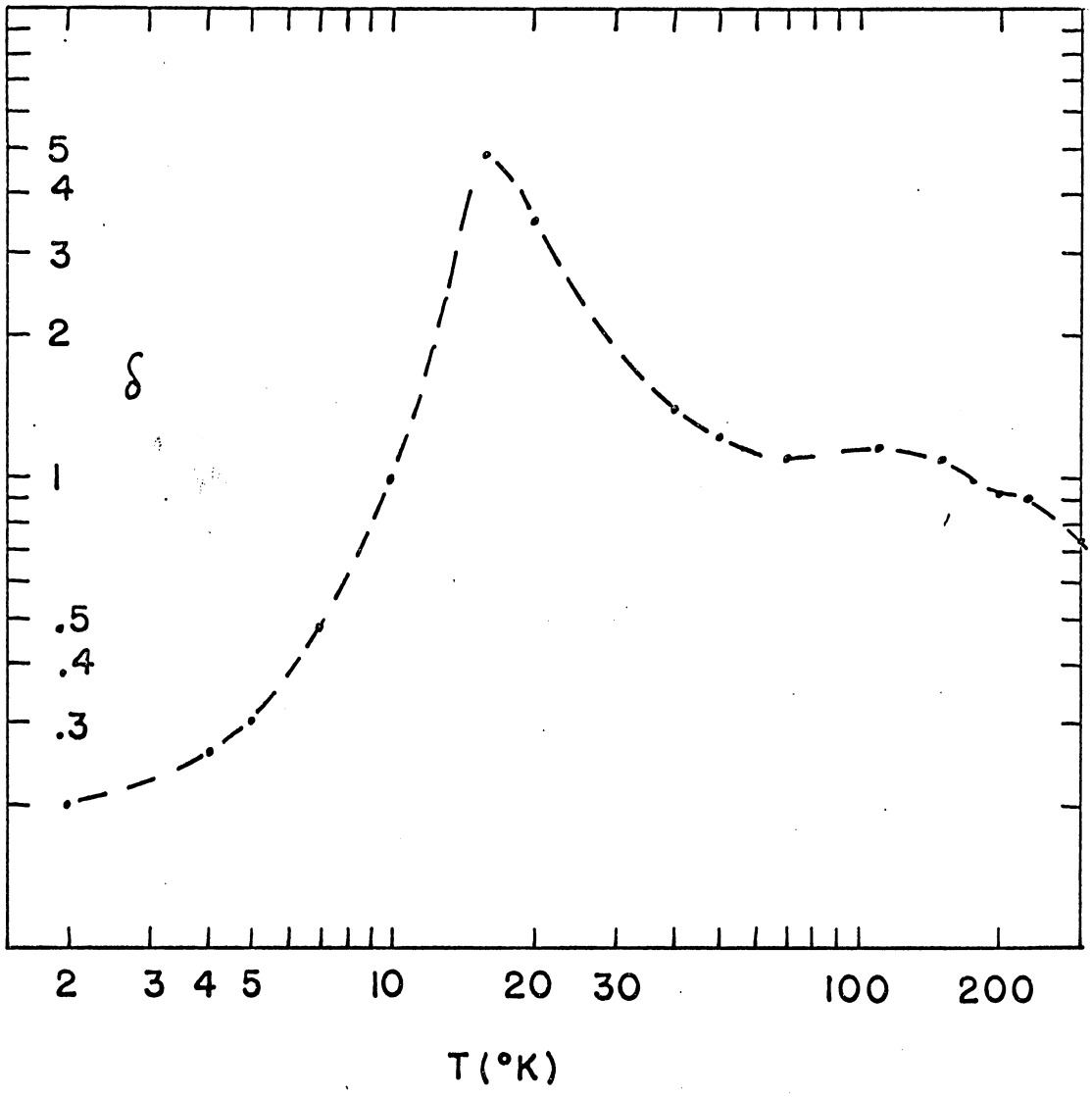

FIGURE 6

BESSEL FUNCTION ARGUMENT δ

continue to decrease with increasing temperature as theory predicts.

It is seen from Figure 5 that the calculated values are lower than the measured values by a factor of 10 at 7°K and a factor of 100 at 2°K. This discrepancy might be due to incorrect estimates of the parameters B and T_2'', resulting in part from the uncertainty in D and T_2. An attempt was made to obtain better agreement between calculated and measured relaxation times. Varying the parameters by orders of magnitude (and recalculating A) showed that better low temperature agreement was possible and also provided initial estimates for an iteration method for the parameters. The iteration method was only partially successful, apparently because the T_1 data could not be fitted simultaneously at 4, 7, and 16 °K using the EPR ρ measurements. However, an improvement is evident from curve c, Figure 5. The final calculation of the iteration forced a fit at 7°K; final values of the parameters are $B = 2.3 \times 10^4\ s^{-\frac{1}{2}}$, $2\pi/T_2'' = 1.4 \times 10^2\ s^{-1}$.

V. Conclusions

Measurements of the F^{19} nuclear spin-lattice relaxation time in CaF_2:Nd reveal a dependence of T_1 on the orientation of the crystal with respect to the magnetic field. This was expected because the diffusion constant D depends on the orientation, as do the g factor and relaxation time of the impurity. Using Rorschach's [5] theoretical expression for T_1, values of the impurity spin-lattice relaxation time were computed from the T_1 data. When compared with EPR measurements and theoretical predictions, the resulting curve is seen to

exhibit the correct qualitative behavior over the entire temperature range, 2°K to 300°K.

In view of approximations made in the development of the nuclear relaxation theory and in the analysis, the agreement between experimental results and the theoretical formula is probably as good as could be expected. The transition probabilities were calculated from simple models using first order perturbation theory; all angles were averaged over; and the barrier radius was only estimated. Possibly, spin diffusion does not cease at the barrier radius that was calculated for another reason: near the impurity second order effects may be important. There is one more possible reason for lack of close agreement between theory and experiment. The doping concentration was low enough that impurities other than neodymium probably have a significant effect.

There are some refinements of the theory which might be profitable. The assumption of a barrier radius within which spin diffuion does not occur and outside of which spin energy diffuses freely is not a very good approximation, and attempts should be made to circumvent this approximation. The averaging over angles which was necessary in order that the magnetization density be a function of r only could be avoided by numerical methods. Consideration of nuclear relaxing mechanisms neglected so far might be helpful. For instance, the neglected dipolar term $S^{\pm}I^{\mp}$ could be significant in some temperature range.

Since in Rorschach's formula, T_1 is dependent on the magnetic field strength H and the impurity concentration N, experiments in which T_1 is measured in crystals differing in N, and experiments in

which H is varied, would further indicate how well the nuclear relaxation time behavior is understood. An investigation of proton relaxation in a single crystal, a hydrate containing Nd^{3+} impurities, in which both H and the temperature were varied, has been carried out at temperatures below $4.2^{o}K$.[14] Analysis employing the rapid diffusion and diffusion limited formulas gave order of magnitude agreement with the experimental results.

VI. Appendices

A. Coefficient of Dipolar Term $S_z I'$

The dipolar interaction between a nuclear spin and an impurity spin is

$$\mathcal{H}_{IS} = \frac{1}{r^3}\left[\bar{\mu}_I \cdot \bar{\mu}_s - 3(\bar{\mu}_I \cdot \hat{r})(\bar{\mu}_s \cdot \hat{r})\right]$$

$$\hat{r} = \frac{\bar{r}}{r} = \alpha_1 \bar{i} + \alpha_2 \bar{j} + \alpha_3 \bar{k}$$

Labeling as z' the impurity axis of axial symmetry, the g tensor in the primed coordinate frame is

$$g' = \begin{pmatrix} g_\perp & 0 & 0 \\ 0 & g_\perp & 0 \\ 0 & 0 & g_{\parallel} \end{pmatrix}.$$

In another frame obtained by rotation through an angle η about the x'-axis

$$g = A\, g' A^{\dagger} \qquad A = \begin{pmatrix} 1 & 0 & 0 \\ 0 & \cos\eta & \sin\eta \\ 0 & -\sin\eta & \cos\eta \end{pmatrix}.$$

Since there is axial symmetry, this is a general rotation because x' can be any direction perpendicular to z'. The magnetic moment vector is then

$$\mu_s = -\beta(g)(S) = -\beta \begin{pmatrix} g_\perp S_x \\ g_b S_y + \Delta g\, S_z \\ \Delta g\, S_y + g_a S_z \end{pmatrix}$$

$$\Delta g = \cos\eta \sin\eta\, (g_{\parallel} - g_\perp)$$

$$g_a = g_\perp \sin^2\eta + g_{\parallel} \cos^2\eta$$

$$g_b = g_\perp \cos^2\eta + g_{\parallel} \sin^2\eta \,.$$

Our interest is in the dipolar term $S_z I^+$, so we retain only terms containing I_x and I_y; thus $\mathcal{H}_{IS}$ takes the form

$$\mathcal{H}_{IS} = -\frac{\gamma\hbar\beta}{r^3}\left[I_y \Delta g\, S_z - 3(\alpha_1 I_x + \alpha_2 I_y) \times (\alpha_2 \Delta g\, S_z + \alpha_3 g_a S_z)\right]$$

Substituting polar coordinates for the direction cosines,

$$\alpha_1 = \sin\theta\cos\phi\,, \quad \alpha_2 = \sin\theta\sin\phi\,, \quad \alpha_3 = \cos\theta$$

and simplifying,

$$\mathcal{H}_{IS} = \frac{\gamma\hbar\beta}{2r^3}\left[i\Delta g + (\Delta g \sin^2\theta\sin\phi + g_a \sin\theta\cos\theta)3e^{-i\phi}\right] S_z I^+ + \text{h.c.}$$

B. Spectral Density of S_z

The spectral density $J(\omega)$ of S_z is related to the correlation function $G(\tau) = \overline{S_z(t)\, S_z(t+\tau)}$, where the bar denotes an ensemble average:

$$J(\omega) = \int_{-\infty}^{\infty} G(\tau)\, e^{-i\omega\tau}\, d\tau\,.$$

Assuming the paramagnetic impurities to be in thermal equilibrium with the lattice, G(0) and G(∞) can be calculated using the Boltzmann distribution. If $\bar{H} \perp z'$,

$$G(0) = \overline{S_z^2} = \sum_{M=\frac{1}{2}}^{-\frac{1}{2}} P_M(M^2) = \tfrac{1}{4}$$

$$P_M = \frac{e^{-E_M/kT}}{\sum_{M'} e^{-E_{M'}/kT}}\,, \qquad E_M = \beta g_\perp M H$$

$$G(\infty) = \sum_{MM'} P_M M\, P_{M'} M' = \left(\sum_M P_M M\right)^2$$

$$= (\overline{S_z})^2 = \tfrac{1}{4}\tanh^2 x\,, \qquad x \equiv \frac{\beta g_\perp H}{2kT}\,.$$

We choose an exponential correlation function consistent with the above conditions,

$$G(\tau) = \tfrac{1}{4}\tanh^2 x + \tfrac{1}{4}(1-\tanh^2 x)\, e^{-|\tau|/\tau_c}$$

In Appendix C it is shown that τ_c is equal to the impurity ion relaxation time ρ. Substituting into the formula for the spectral density and carrying out the integration,

$$J(\omega) = 2\pi \tfrac{1}{4}\tanh^2 x\, \delta(\omega) + \tfrac{1}{4}(1-\tanh^2 x)\, \frac{2\tau_c}{1+\tau_c^2\omega^2}.$$

C. Equality of the Correlation Time and the Impurity Relaxation Time

For small τ the correlation function can be calculated. Letting $P_{1/2}$ be the probability of spin 1/2, and letting $W_\uparrow$ be the probability per second for the spin transition $-1/2 \rightarrow 1/2$,

$$\begin{aligned} G(\tau) &= \overline{S_z(0)\, S_z(\tau)} \\ &= [\tfrac{1}{2} P_{\frac{1}{2}}][(W_\downarrow \tau)(-\tfrac{1}{2}) + (1-W_\downarrow)(\tfrac{1}{2})] \\ &\quad + [(-\tfrac{1}{2}) P_{-\frac{1}{2}}][(W_\uparrow \tau)(\tfrac{1}{2}) + (1-W_\uparrow)(-\tfrac{1}{2})]. \end{aligned} \qquad (1)$$

ρ can be expressed in terms of $W_\uparrow$ and $W_\downarrow$, and these two transition probabilities are related to each other. First,

$$\frac{d P_{\frac{1}{2}}}{dt} = P_{-\frac{1}{2}} W_\uparrow - P_{\frac{1}{2}} W_\downarrow \qquad (2)$$

and the observed impurity magnetization is proportional to

$$m = P_{\frac{1}{2}} - P_{-\frac{1}{2}} = 2P_{\frac{1}{2}} - 1 .$$

$$\frac{dm}{dt} = 2\frac{dP_{\frac{1}{2}}}{dt}$$

$$= -m(W_\uparrow + W_\downarrow) + (W_\uparrow - W_\downarrow) \quad \text{after algebraic manipulation.}$$

Introducing the equilibrium magnetization

$$\frac{dM}{dt} = -(W_\uparrow + W_\downarrow)(M - M_0) .$$

Therefore, by definition of the relaxation time,

$$\rho = \frac{1}{W_\uparrow + W_\downarrow} . \qquad (3)$$

At equilibrium, $P_{1/2}$ and $P_{-1/2}$ are related by the Boltzmann distribution. We then obtain from equation (2)

$$\frac{W_\uparrow}{W_\downarrow} = \frac{P_{1/2}}{P_{-1/2}}\Big)_0 = e^{-2x} \qquad (4)$$

$$x = \frac{\beta g_1 H}{2kT}$$

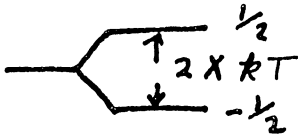

Applying equations (3) and (4) to the expression (1) for $G(\tau)$ and simplifying,

$$G(\tau) = \tfrac{1}{4} - \frac{\tau}{4\rho} \operatorname{sech}^2 x .$$

Returning to the assumed correlation function of Appendix B, we can expand the exponential for small τ,

$$G(\tau) = \tfrac{1}{4} \tanh^2 x + \tfrac{1}{4}(1 - \tanh^2 x)\, e^{-|\tau|/\tau_c}$$

$$= \tfrac{1}{4} \tanh^2 x + \tfrac{1}{4}(1 - \tanh^2 x)\left(1 - \tfrac{\tau}{\tau_c}\right)$$

$$= \tfrac{1}{4} - \tfrac{1}{4} \frac{\tau}{\tau_c} \operatorname{sech}^2 x .$$

This is exactly the same as the calculated expression with ρ replaced by τ_c, the correlation time.

D. Effective Impurity Magnetic Moment

To estimate the static moment μ_e of the paramagnetic impurity effective in quenching spin diffusion, we begin with the definitions of the correlation function $K(\tau)$ and the spectral density $J(\omega)$.

$$K(\tau) = \overline{\mu_z(t)\,\mu_z(t+\tau)} = \frac{1}{2\pi}\int_{-\infty}^{\infty} J(\omega)\, e^{i\omega\tau}\, d\omega .$$

By Fourier inversion

$$J(\omega) = \int_{-\infty}^{\infty} K(\tau)\, e^{-i\omega\tau}\, d\tau .$$

Thus the ensemble average of the square of the magnetic moment is resolved into spectral components,

$$\overline{\mu_z^2} = K(0) = \frac{1}{2\pi}\int_{-\infty}^{\infty} J(\omega)\, d\omega .$$

Frequencies effective in quenching diffusion have a period $\frac{1}{\nu} > T_2''$. T_2'' is the mean lifetime of a nucleus against spin diffusion. We can now find μ_e:

$$\mu_e^2 = \frac{1}{2\pi}\int_{-\frac{2\pi}{T_2''}}^{\frac{2\pi}{T_2''}} J(\omega)\, d\omega .$$

From Appendix A, if $\bar{H} \perp z'$,

$$\mu_z = -\beta g_\perp S_z$$

$$\therefore\ J(\omega) = (\beta g_\perp)^2 J(\omega)$$

$$\cong (\beta g_\perp)^2 \left(2\pi \tfrac{1}{4} \chi^2 \delta(\omega) + \tfrac{1}{4} \frac{2\rho}{1+\rho^2\omega^2}\right)$$

The approximation is very good for temperatures greater than 2°K. Carrying out the integration,

$$\mu_e^2 = \left(\frac{\beta g_\perp}{2}\right)^2 \left(\chi^2 + \frac{2}{\pi} \tan^{-1} \frac{2\pi\rho}{T_2''}\right) .$$

Acknowledgments

I would like to thank Dr. Harold E. Rorschach for his direction of this thesis work. I am also grateful for the aid extended by fellow graduate students. This research was supported in part by the National Aeronautics and Space Administration and by the Office of Naval Research.

References

1. N. Bloembergen, Physica 15, 386 (1949)
2. G. R. Khutsishvili, Soviet Phys. JETP 15, 909 (1962)
3. P. G. De Gennes, J. Phys. Chem. Solids 7, 345 (1958)
4. W. E. Blumberg, Phys. Rev. 119, 79 (1960)
5. H. E. Rorschach, Physica 30, 38 (1964)
6. M. J. Weber, R. W. Bierig, Phys. Rev. 134, A1492 (1964)
7. M. A. Waldrop, Ph.D. Thesis, Rice University, Houston, Texas (1963)
8. A. Abragam, The Principles of Nuclear Magnetism, Oxford University Press (1961)
9. C. P. Slichter, Principles of Magnetic Resonance, Harper and Row (1963)
10. J. M. Dauphinee, D. K. C. MacDonald, W. B. Pearson, J. Sci. Instrum. 30, 399 (1953)
11. H. van Dijk, M. Durieux, Progress in Low Temperature Physics and Chemistry, vol. 2, edited by C. J. Gorter, North Holland, (1957), p. 431
12. C. B. P. Finn, R. Orbach, W. P. Wolf, Proc. Phys. Soc. 77, 261 (1961)
13. R. Orbach, Proc. Phys. Soc. 77, 821 (1961)
14. C. D. Jeffries, Dynamic Nuclear Orientation, Interscience Publishers (1963)